



Parasitic Egg Detection and Classification in Low-Cost Microscopic Images Using Transfer Learning

Thanaphon Suwannaphong¹ · Sawaphob Chavana² · Sahapol Tongsom² · Duangdao Palasuwan³ · Thanarat H. Chalidabhongse² · Nanthheera Anantrasirichai⁴

Received: 7 July 2022 / Accepted: 10 October 2023
© The Author(s) 2023

Abstract

Intestinal parasitic infection leads to several morbidities in humans worldwide, especially in tropical countries. The traditional diagnosis usually relies on manual analysis from microscopic images which is prone to human error due to morphological similarity of different parasitic eggs and abundance of impurities in a sample. Many studies have developed automatic systems for parasite egg detection to reduce human workload. However, they work with high-quality microscopes, which unfortunately remain unaffordable in some rural areas. Our work thus exploits a benefit of a low-cost USB microscope. This instrument however provides poor quality images due to the limitation of magnification (10×), causing difficulty in parasite detection and species classification. In this paper, we propose a CNN-based technique using transfer learning strategy to enhance the efficiency of automatic parasite classification in poor-quality microscopic images. The patch-based technique with a sliding window is employed to search for the location of the eggs. Two networks, AlexNet and ResNet50, are examined with a trade-off between architecture size and classification performance. The results show that our proposed framework outperforms the state-of-the-art object recognition methods. Our system combined with the final decision from an expert may improve the real faecal examination with low-cost microscopes.

Keywords Human intestinal parasites · USB microscope · Automatic detection · Deep learning · Convolutional neural networks · Transfer learning

Introduction

Intestinal parasitic infection leads to several morbidities such as diarrhea digestive disorders, malnutrition, anemia or even death to humans worldwide, especially in tropical countries [1]. There are more than 100 different species of human

intestinal parasites [2] that can grow with a considerably rapid rate of 200,000 eggs re-produced daily [3]. Indubitably, over 415,000 human deaths due to parasite infestation are reported annually [4]. The conventional methods to diagnose intestinal parasitic infection depend exclusively on medical technicians in microscopic examinations of faecal samples. The potential problems are morphological similarity of parasites and abundance of impurities in a sample, causing a difficulty to manually inspect different types of parasite eggs via a microscope [3, 5]. This thus requires extensive training to gain adequate expertise in diagnosis. This examination is laborious and time-consuming, averaging 8–10 mins required for an expert technician to examine one sample [4]. In addition, the lack of skilled workers in this field leads to exhaustion, which means this method is prone to human errors [6]. Moreover, these conventional methods do not provide a data-sharing system and record historical data of diagnosis. For these reasons, the invention of an automated diagnostic system would become a significant contribution to assist the traditional diagnosis.

✉ Thanaphon Suwannaphong
ic19511@bristol.ac.uk

✉ Nanthheera Anantrasirichai
n.anantrasirichai@bristol.ac.uk

¹ Department of Engineering Mathematics, University of Bristol, Bristol, UK

² Department of Computer Engineering, Chulalongkorn University, Bangkok, Thailand

³ Research Group on Applied Computer Engineering Technology for Medicine and Healthcare, Chulalongkorn University, Bangkok, Thailand

⁴ Visual Information Laboratory, University of Bristol, Bristol, UK

Since the development of image processing techniques and computer vision, the automated diagnosis systems have become more feasible. Many studies have implemented the systems to analyse microscopic image of faecal samples based on machine learning, e.g. support vector machine (SVM) [7, 8] and artificial neural networks (ANN) [5, 7]. The core components of these systems commonly include pre-processing, feature extraction and classification to identify species of parasitic eggs. The approaches generally consider the difference in the external features such as size, shape and smoothness of eggshell. These traditional machine learning approaches do not require very complex designs; however, they rely heavily on the selectively extracted features. This means a tremendous effort is needed for tuning the features in feature extraction stage.

In the last decade, as computer performance and quantity of available image datasets have both increased, the deep learning-based algorithms have rapidly become more popular [9]. Deep learning shows high efficiency to tackle problems in many different domains, such as text recognition, computer-aided diagnosis, face recognition and drug discovery [10]. In the parasite egg detection task, deep learning, especially the convolutional neural networks (CNNs), motivates novel parasite classification research by its promising performance and speed in object detection [4, 6, 11–14]. CNNs have an advantage to avoid manual feature extraction by using its ability to learn the relevant features automatically from a large amount of data that represents the desired behaviour of the data [15]. CNNs have demonstrated high accuracy in numerous different tasks of pathogen detection such as malaria, tuberculosis, and intestinal parasite [6]. With this approach, the intestinal parasite diagnosis can be independent of the experts, save time, increase sensitivity, and hopefully be used on-site.

Previous automatic systems proposed for the parasite egg detection have employed high-quality microscopes (1000 \times). These instruments are expensive and have limited availability in rural areas. Therefore, we are motivated to employ a low-cost USB microscope in this paper. It comes with low magnification (10 \times), generating poorer image quality as shown in Fig. 1. At high resolutions (high magnification), the images of different parasite species show unique characteristics and textural patterns inside the eggs (left images). This aids the CNNs to learn these expressed image patterns and assists identifying the parasite species. In contrast, the images from low magnification contain obviously fewer characteristics and pattern details of the parasitic eggs, leading to difficulty in detection and species classification.

This paper addresses these challenges by applying a transfer learning technique with pretrained CNN networks (Fig. 2). Our proposed framework starts with image processing to enhance the image quality. We subsequently

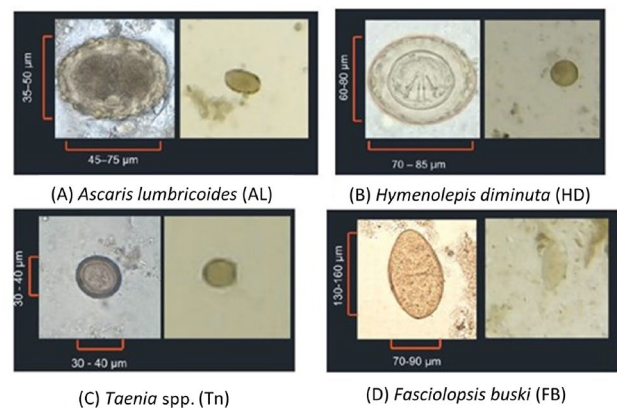


Fig. 1 The comparison of parasitic egg images from (left) good quality microscope and (right) USB microscope

employ the transfer learning strategy and test two pretrained networks: AlexNet [16] and ResNet50 [17], to examine a trade-off between the lighter-weight architecture and better classification performance. These two well-known networks were used because they were trained on large datasets, acquiring rich and generalisable feature representations. They also allow for faster convergence during fine-tuning on our task. Our detection technique is a patch-based sliding window, where the unlabelled microscopic images are separated into overlapping patches, fed to the trained model, and the location of the detected egg is where the maximum probability of being parasite egg is. Our proposed automated system based on supervised deep learning shows potential to enhance the efficiency of automatic parasite egg detection and classification in poor-quality microscopic images that have never been investigate in the state of the art. Obviously, there is a difficulty to identify parasite species from these USB microscopic images; however, our system could be a preliminary diagnostic tool before the next process for species identification can be performed for more specific species classification.

Materials and Methods

Parasite Eggs in USB Microscopic Images

Our dataset contains 10 \times magnification microscopic images with a resolution of 640 \times 480 pixels. Four different types of parasitic eggs present: 67 images of *Ascaris lumbricoides* (AL), 27 images of *Hymenolepis diminuta* (HD), 32 images of *Fasciolopsis buski* (FB) and 36 images of *Taenia* spp. (Tn). The images were obtained from Chulalongkorn University, Thailand, and were labelled by experts. The limitation of the low magnification causes difficulty in species identification because of the lack

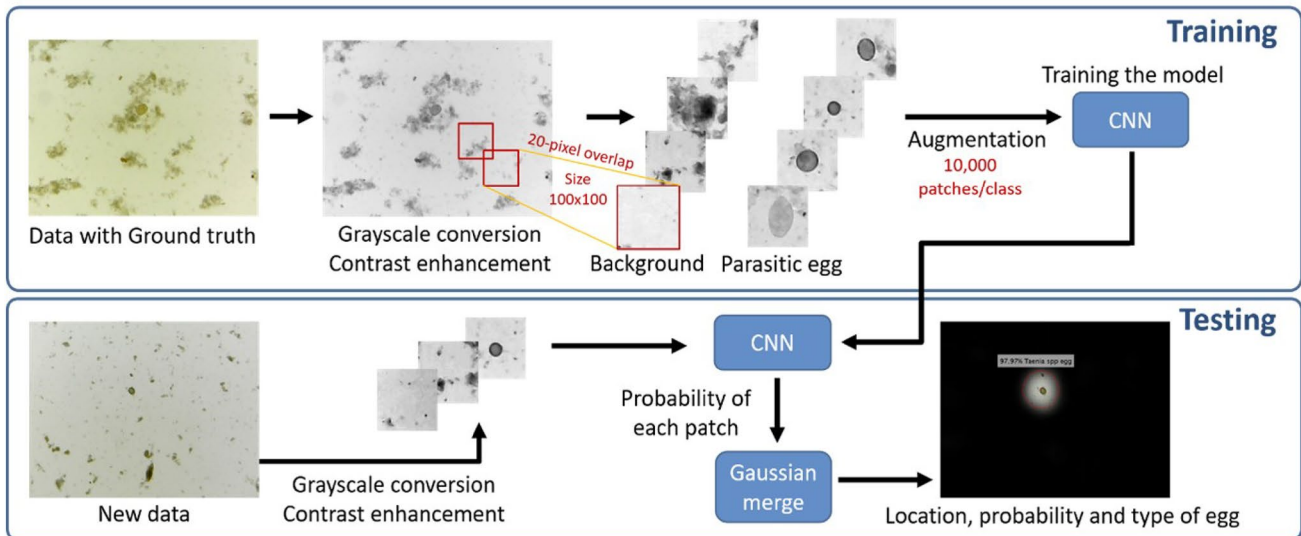


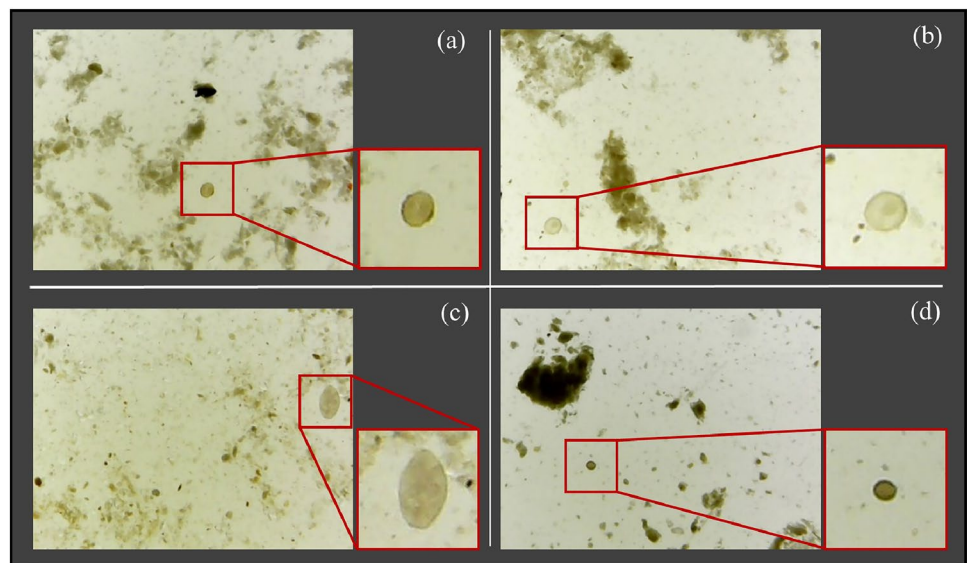
Fig. 2 Diagram of the proposed framework for training and testing CNN model

of details of the parasitic eggs present in the images as shown in Fig. 3. The AL is the most common roundworm in humans [2]. The egg appearance is generally round but slight oval shapes are also found (Fig. 3a) with varied degrees of ellipticity. The HD eggs under the USB microscope look very similar to the AL eggs but the HD eggs are generally more circular than the AL eggs (Fig. 3b). Figure 3c shows a large parasitic egg, *Fasciolopsis buski*, of which the detail showed is very low. The parasitic egg in Fig. 3d shows common characteristics of *Taenia* eggs but the egg detail is not enough to specify the *Taenia* species. So, the experts classify these eggs as *Taenia* spp.

Data Preparations

Greyscale conversion and contrast enhancement are performed before processing the patch overlapping and data augmentation. The greyscale conversion reduces the depth of the input image from three channels (RGB) to one channel (greyscale), diminishing the computational complexity of the training process. The contrast enhancement improves visualisation of the low-magnification microscopic images. This aids the CNN model to detect the low-level features, like edges and curves, and contributes to the detection performance of higher-level features, like characteristics of parasitic eggs.

Fig. 3 USB microscopic images of 4 types of parasitic eggs **a** *Ascaris lumbricoides* **b** *Hymenolepis diminuta* **c** *Fasciolopsis buski* and **d** *Taenia* spp.



Overlapping Patches

Each microscopic image is divided into patches, allowing the model to characterise the whole image by analysing local areas. The largest parasite egg is approximately 80×20 pixels. The patch size is thus defined to be 100×100 pixels so that all types of parasitic egg can be entirely encapsulated. The positions of patches overlap by four-fifths of the patch size as shown in Fig. 4. This empirical choice provides a good prediction result when merging the probability of all patches together to reconstruct the probability map corresponding to the input microscopic image. To label the training dataset, the patch that contains a parasite egg is labelled as an egg patch, whilst the patch without parasite egg is labelled as the background.

Data Augmentation

Generally each microscopic image contains only 1–3 eggs, resulting highly imbalanced training dataset as there are numerous background patches. Data augmentation is therefore employed to increase the number of egg patches and to balance the number of patches in each class. This approach also ensures that data points are positioned to prevent overfitting. The augmentation increases the variance of the training dataset, which makes the model invariant to location and orientation of eggs presenting in each patch. In this work, we generate more egg patches by (i) randomly flipping horizontally and vertically, (ii) randomly rotating between angle of 0 to 160 degrees, and (iii) randomly shifting every 50 pixels horizontally and vertically around the egg. This data augmentation technique increases the egg patches to approximately 10,000 patches per egg type. We randomly select 10,000 background patches so that the numbers are balanced.

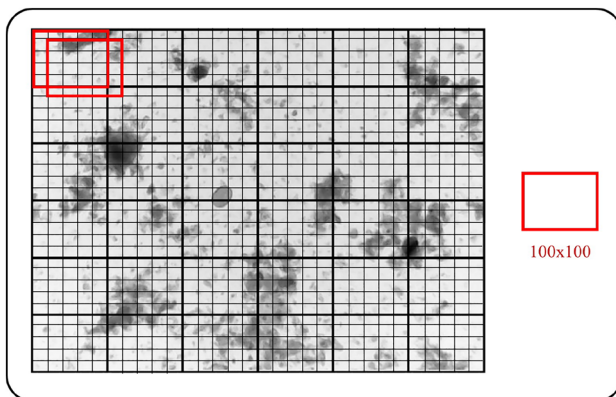


Fig. 4 Patch overlapping technique

Methods with Transfer Learning

We employ a transfer learning strategy by fine-tuning pre-trained networks. This approach is faster and easier than training a network with randomly initialised weights from scratch. Parameters and features of these networks have been learnt from a very large dataset of natural images thereby being applicable to numerous specific applications. The last two layers are replaced with a fully connected layer and a softmax layer to give a classification output related to five classes: 4 parasite egg types and background debris. The learning rates of the new layers are defined to be faster than the transferred layers.

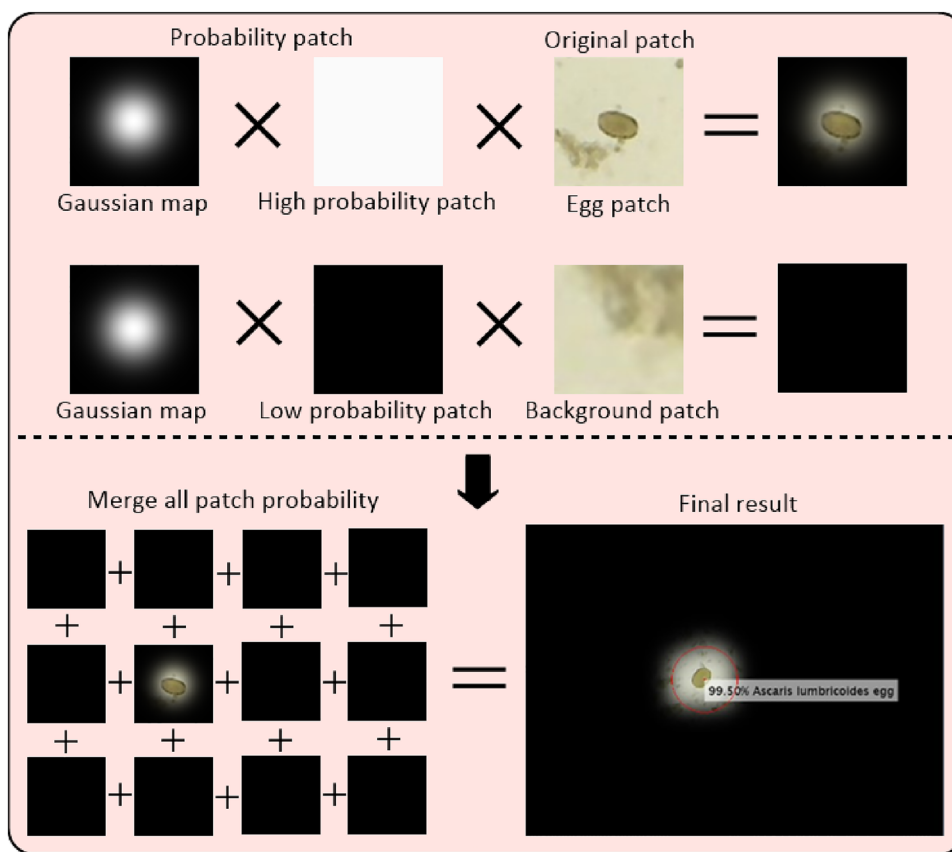
Two pretrained networks are tested, i.e. AlexNet [16] and ResNet50 [17], in order to examine a trade-off between network size and classification performance. AlexNet is a pioneer model that has significantly contributed to the CNN performance for object recognition, whilst ResNet50 is more modern, deeper architecture and generally gives better performance on image classification.

The prepared patches as described in the previous step are resized to the input size required for each network, i.e. 227×227 and 224×224 pixels for AlexNet and ResNet50, respectively. We randomly choose 30 percent of the training patches for validation in the training process. The initial learning rate, mini-batch size, and maximum epochs are varied to find the optimal setting. The data was shuffled every epoch to avoid creating a bad mini batch which is a poor representation of the overall dataset. We select the best model from the first model that provided the lowest validation loss to avoid overfitting.

Prediction Process

The testing microscopic images are processed with grey-scale conversion, contrast enhancement, and patch overlapping process using the same parameters as the training dataset. Each patch in an image is classified using the trained models which provide the probability of each overlapping patch to identify the type of parasite eggs or background debris. The classification result of each patch gives five probability values of being AL, HD, FB, Tn and background. The final prediction result of the whole image comes from the maximum value of these five probabilities among all overlapping patches of the whole image. We combine the probability values of all overlapping patches to construct the probability map of the whole image as shown in Fig. 5. We achieve this by multiplying the probabilities of every overlapping patch with Gaussian weights ($\mu = 0$, $\sigma = 1$, where μ and σ are the mean and the standard deviation, respectively), and then summing up the probabilities of overlapping pixels too reconstruct the probability map of the whole image. As we employed a patch-based technique,

Fig. 5 Final probability map generation. We create the image’s probability map by multiplying each patch’s probability with Gaussian weights and summing these values at overlapping pixels. The parasite egg’s location corresponds to the patch with the highest probability of being an egg



the localised information is derived from the patch’s location (Fig. 5 bottom part). Therefore, the location of the detected parasite egg is the location of the patch that provides the highest probability values of being a parasite egg.

Experimental Results and Discussion

The dataset of each parasitic egg type is divided into training and testing with a ratio of 60:40. So, the testing dataset consists of 65 images: 27 AL, 11 HD, 13 FB, and 14 Tn images. In the fine-tuning process, two optimisers were compared: stochastic gradient descent with momentum (SGDM) and Adaptive Moment Estimation (Adam). The initial learning rate was varied: 0.001, 0.0001 and 0.00001. The mini-batch size varied between 20, 50 and 100. For both AlexNet and ResNet50, we found that the SGDM optimiser with the initial learning rate of 0.0001, the mini-batch size of 100, and 20 epochs gave the best result (achieving the training accuracy of 93.95% and 99.80% for AlexNet and ResNet50, respectively). It should be noted that the results of using a pretrained model and a non-pretrained model showed insignificant differences in performance, but the training speed was approximately three times faster with the pretrained model. While pretrained models are expected to help in

generalisation and reduce the risk of overfitting, unfortunately we could not verify this on our limited dataset.

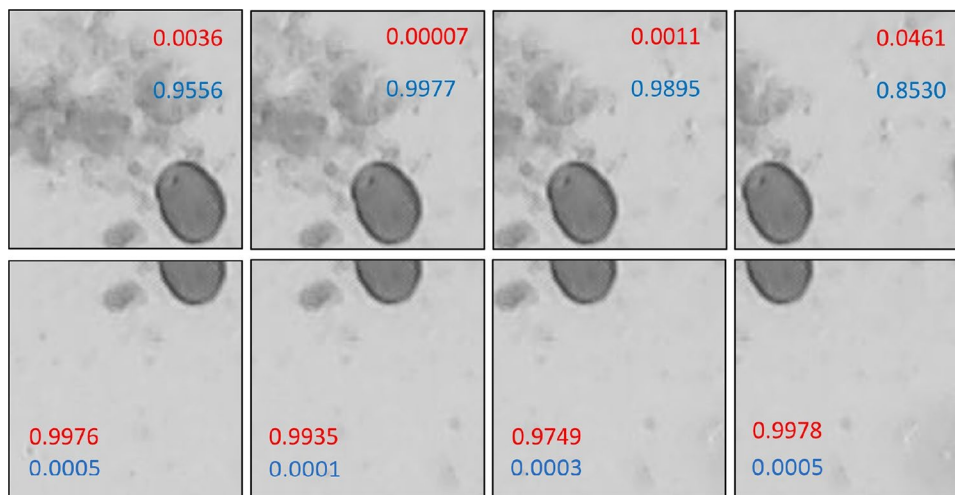
The validation in the training process shows that both models can classify background patches with 100% accuracy. For the AL patches, the ResNet50 only shows one misclassified patch to be a background patch whereas AlexNet produces more misclassified patches as background as well as misclassified patches to be other types of eggs. ResNet50 identifies HD patches with no mistake while AlexNet shows 7% misclassified HD patches. The FB patches are the most difficult to identify because FB eggs have very low contrast, making it less noticeable compared to other parasitic eggs. Unsurprisingly, the AlexNet performance to classify the FB patches is relatively low compared to other types of eggs. However, the ResNet50 provides an impressive result in FB patch classification with an interestingly high accuracy of 93.50%. In the same way, ResNet50 also gives a better result than AlexNet for the Tn patches.

Classification Results

In the testing process of classification, the true positive rate is relatively low when analysing each patch separately for both models, as reported in Table 1 with an analysis type of ‘patch’. Several egg patches are classified as background

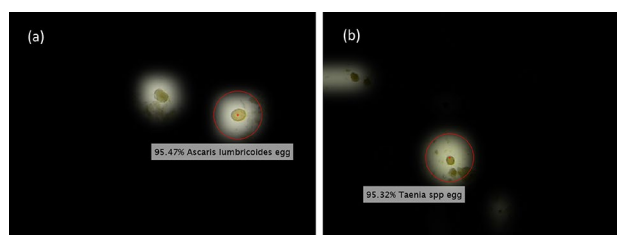
Table 1 Testing results of AlexNet and ResNet50 models

Models	Analysis type	Accuracy (%)	True positive rate (%)				True negative rate (%)
			AL	HD	FB	Tn	
AlexNet	Patch	96.93	45.45	34.23	19.92	53.76	99.23
	Whole image	87.69	96.30	81.82	76.92	85.71	–
ResNet50	Patch	98.25	64.09	73.42	56.39	73.48	99.57
	Whole image	90.77	92.59	81.82	100.00	85.71	–

Fig. 6 Examples of testing result for egg patches. Red values represent the probability of the patch being background debris. Blue values represent the probability of the patch to be an AL egg

(the highest probability is given to the background class). Most of these patches have an egg located at the edge of the patches—in other words, only a partial egg presents in the patches as displayed in Fig. 6. In the detection process, the probabilities of overlapping patches are merged into the probability map of the testing microscopic image. This results in an increase in the probability of there being a parasitic egg in the egg area. As a result, the true positive rates increase when analysing the whole image (Table 1 with analysis type of ‘whole image’). Overall, the ResNet50 model outperforms the AlexNet one in all egg cases, measured by the accuracy, true positive and true negative rates. The true negative rates are very high for the patch analysis of both AlexNet and ResNet50—background patches are classified as background. Unfortunately, we cannot determine the true negative rates for whole image analysis because we do not have any microscopic images containing only debris (no parasite eggs) to test the model.

Figure 7 shows some false positives in the detection results of AlexNet. These areas have smaller probability values than the correctly detected areas in other images. The ResNet50 model yields better results than the AlexNet model as shown in the confusion matrices of Fig. 8. Interestingly, the ResNet50 model achieves 100% accuracy of FB detection (Fig. 8d), which is the most

**Fig. 7** AlexNet confusion results: **a** detected AL egg correctly (red area) but also included the debris which have similar morphology as AL egg (left bright area), **b** detected Tn egg correctly (red area) but also detect debris as Tn egg with a lower probability (left dim area)

challenging egg in this study due to the low contrast and lack of details inside the eggs. This can be seen via the result of the patch analysis, where the FB patches yield the lowest accuracy because almost half of FB patches are classified as background debris (Fig. 8c). In addition, the ResNet50 generally gives higher probability than the AlexNet for either being parasite eggs or background debris, indicating more confidence in prediction. In some images, neither AlexNet nor ResNet50 can detect any parasite eggs. However, these egg areas have significantly lower probability values of being background than other parts of the image (Fig. 9).

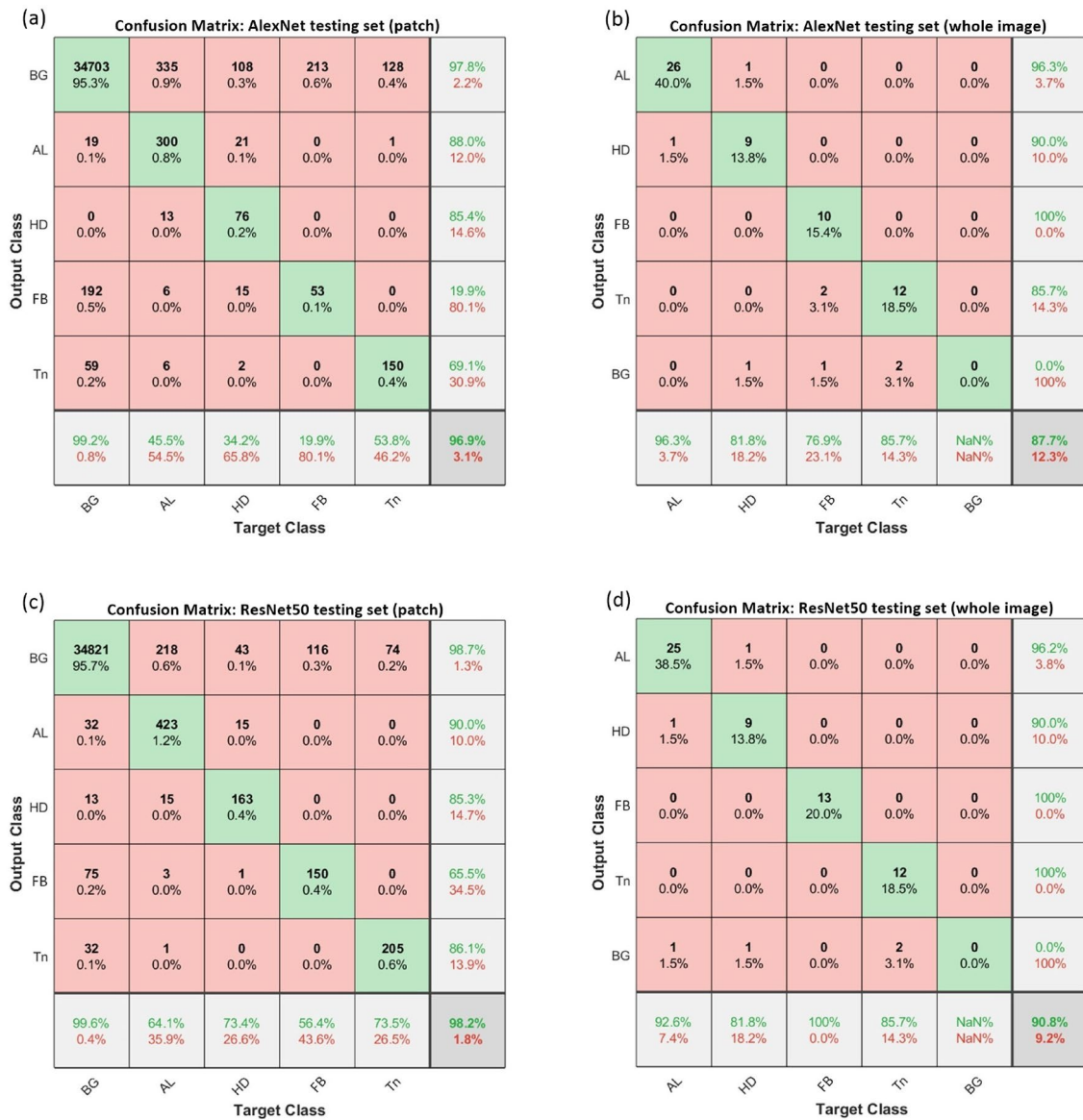


Fig. 8 Confusion matrices from the testing process

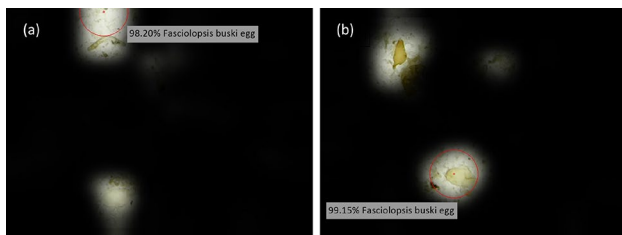


Fig. 9 Examples of ResNet50 testing results for FB egg. **a** the debris in the upper bright area shows a higher probability than the FB egg in the lower bright area. **b** the debris at the upper bright area shows a lower probability than the FB egg in the lower bright area

Comparison with State-of-the-Art Object Detection

We compared our methods with two state-of-the-art object detection methods: Single shot detector (SSD) [18] and Faster R-CNN [19]. SSD is a very light-weight network having one single shot to detect multiple objects within the image, whilst Faster R-CNN requires two shots, one for searching for regions of interest (ROI), and the other for detecting the object in each ROI using CNNs. The backbones of SSD and Faster R-CNN used here are VGG-16 and ResNet50 architectures, respectively. It is worth to mention that You Only Look Once (YOLO) [20], a state-of-the-art real-time object detection, is not suitable for

our application. This is because YOLO struggles to detect small objects within the image.

Table 2 shows the precision results of our methods compared to SSD and Faster R-CNN. The precision, or positive predictive value (PPV), indicates the percentage of correctly identified eggs from all detected eggs in one particular egg type. The proposed method with the ResNet50 gives the best average precision, followed by Faster R-CNN. Our AlexNet model outperforms SSN despite its smaller architecture and fewer parameters. Our method exploits a sliding window technique which works really well in this application. This is because the size of each patch can be fixed, and the aspect ratio of the objects we want to detect (parasite eggs) is not present in various shapes, unlike natural images that contain people, cars and buildings. The adaptive size of a bounding box, as offered by SSD and Fast R-CNN, does not benefit parasite egg detection. Moreover, background of the microscopic image does not contain useful information; it is generally just homogeneous and noisy. This is different from natural images, where the background informs what objects are likely to be located there.

Test with Different Dataset

Our proposed method was rigorously evaluated on a substantial dataset, Chula-ParasiteEgg-11 [21], which was used in the ICIP 2022 Challenge. This dataset consists of 11 different types of parasitic eggs, exhibiting variations in sizes. For each parasitic egg type, 1250 images were obtained from 5 different devices. Note that these devices are not low-cost microscopic images and have higher quality than our dataset. 1000 images from each class were allocated for training, while the remaining 250 images were reserved for testing. To facilitate robust evaluation, we applied our data preparation scheme, involving overlapping patches and data augmentation. Notably, in this new dataset, we altered the patch size to 300×300 pixels from the previous 100×100 pixels to effectively capture the various sizes of the parasitic eggs.

The experimental findings demonstrated that AlexNet and ResNet50 achieved average precision values of 65.08% and 73.65%, respectively, across all 11 types of parasitic eggs. These precision values, although commendable, were

relatively lower when compared to the results obtained with our previous dataset. This is because the Chula-ParasiteEgg-11 dataset is significantly larger and more diverse in terms of the devices used and the image magnification.

Discussion

The CNNs can automatically learn relevant useful features even in microscopic images with poor magnification. The transfer learning technique is a very efficient method that has the capability to produce high-performance parasite egg detection within a short time. However, the transferred model requires an optimal parameter setting for the training process to yield the best result. We found that training the model with too many epochs, e.g. 50 or 100 epochs, may result in an overfitting problem, where the model provides extremely high accuracy for a training result, but the testing accuracy is extremely poor. Therefore, early stopping techniques are required or validation loss is monitored as we employ in this paper.

The proposed frameworks, especially the model based on ResNet50, achieve a satisfactory result for parasite detection task with a sufficiently high accuracy in classifying the testing images. The model has the remarkable ability to locate a parasite egg position and identify species of the parasite egg correctly even in a low-quality microscopic image. The ResNet50 model outperforms AlexNet and SSD because of its deeper architecture, leading to better handling of the variation and non-linearity of data. The deeper networks can learn complex features. Misclassified results still occur but if we combine the prediction result of the model with the final decision from an expert, this will improve the diagnosis of parasite infection disease. However, the poor-quality microscopic image with insufficient detail is still a big challenge that prevents the model from correctly discriminating between different types of parasite eggs and sample impurities. Thus, more work is still required to improve this system.

Despite the high classification performance of the model, misclassification remains. A larger pretrained network may help the model to learn more complex features of the parasite eggs. Semantic segmentation, e.g. U-Net [22, 23] might be employed to label the ground truth more precisely. This may aid the model to extract the relevant features more accurately.

When testing with the Chula-ParasiteEgg-11 dataset, the accuracy drops due to its diversity. In particular, the same parasitic egg image, when viewed at different magnifications with the same patch size, exhibited discernible differences, affecting the method's classification performance. To address this inherent limitation, adaptively adjusting the patch size corresponding to the image magnification could be employed. The suitable patch size could captures the relevant features of parasitic eggs accurately.

Table 2 Comparison with stat-of-the-art object detection

Models	Precision (%)				Avg.
	AL	HD	FB	Tn	
SSD	86.7	85.1	73.3	67.3	78.1
Faster R-CNN	92.5	97.3	98.9	95.8	96.1
Our AlexNet	96.3	90.0	100	85.7	93.0
Our ResNet50	96.2	90.0	100	100	96.6

Bold indicates the best performance

Despite this limitation, our method remains robust and highly effective for the majority of parasitic egg types. The precision rates for eight out of the eleven classes ranged from 65 to 93% with ResNet50, indicating substantial success in egg-type classification. While the precision rates for the three classes, *Capillaria philippinensis*, *Fasciolopsis buski*, and *Hymenolepis nana* eggs, were limited to 50–60% with ResNet50, we believe that further optimization and fine-tuning could potentially yield improved results for these specific classes.

Conclusions

This paper presents a deep learning technology with a transfer learning approach for an automatic system of parasite egg detection and classification during a faecal examination. The proposed CNN models show a competent ability in learning relevant features of the different parasitic eggs even in low-quality images sourced from a USB microscope. Overall, our ResNet50 framework can classify the four types of parasitic eggs with high accuracy and outperforms AlexNet, SSD and Faster R-CNN. With this satisfactory result, this approach may be performed with real faecal examination with USB microscopes. The proposed framework is also robust when dealing with data containing a larger number of categories and high diversity, achieving a precision of 75–93% in the majority of parasitic egg types of Chula-ParasiteEgg-11 dataset.

Acknowledgements This work was supported by Newton Fund Institutional Links [grant number 623714323] and a scholarship from Royal Thai Government under the Ministry of Higher Education, Science, Research and Innovation.

Data Availability The datasets generated and analysed during the current study are available from the corresponding author upon reasonable request.

Declarations

Conflict of Interest The authors declare that we have no known competing financial interests or personal relationships that could have appeared to influence the work reported in this paper.

Open Access This article is licensed under a Creative Commons Attribution 4.0 International License, which permits use, sharing, adaptation, distribution and reproduction in any medium or format, as long as you give appropriate credit to the original author(s) and the source, provide a link to the Creative Commons licence, and indicate if changes were made. The images or other third party material in this article are included in the article's Creative Commons licence, unless indicated otherwise in a credit line to the material. If material is not included in the article's Creative Commons licence and your intended use is not permitted by statutory regulation or exceeds the permitted use, you will need to obtain permission directly from the copyright holder. To view a copy of this licence, visit <http://creativecommons.org/licenses/by/4.0/>.

References

1. Yami A, Mamo Y, Kebede S. Prevalence and predictors of intestinal helminthiasis among school children in Jimma zone; a cross-sectional study. *Ethiop J Health Sci*. 2011;21(3):167–74.
2. Ghazali K, Alsameraai R, Mohamed Z. Automated system for diagnosis intestinal parasites by computerized image analysis. *Mod Appl Sci*. 2013;7:98–114.
3. Hadi R, Ghazali K, Khalidin I, Zeehaida M. “Human parasitic worm detection using image processing technique,” *2012 International Symposium on Computer Applications and Industrial Electronics (ISCAIE)*, 2012;pp. 196–200.
4. Holmstrom O, Linder N, Ngasala B, Martensson A, Linder E, Lundin M, Moilanen H, Suutala A, Diwan V, Lundin J. Point-of-care mobile digital microscopy and deep learning for the detection of soil-transmitted helminths and schistosoma haematobium. *Glob Health Action*. 2017;10:49–57.
5. Yang Y, Park D, Kim H, Choi M, Chai J. Automatic identification of human helminth eggs on microscopic fecal specimens using digital image processing and an artificial neural network. *IEEE Trans Biomed Eng*. 2001;48:718–30.
6. Quinn J, Nakasi R, Mugagga P, Byanyima P, Lubega W, Andama A. Deep convolutional neural networks for microscopy-based point of care diagnostics. *Mach Learn Health Care Conf*. 2016;56:271–81.
7. Ray K, Shil S, Saharia S, Sarma N, Karabasanavar N. Detection and identification of parasite eggs from microscopic images of fecal samples. *Comput Intell Pattern Recogn*. 2020. https://doi.org/10.1007/978-981-13-9042-5_5.
8. Avci D, Varol A. An expert diagnosis system for classification of human parasite eggs based on multi-class SVM. *Expert Syst Appl*. 2009;36:43–8.
9. Goodfellow I, Bengio Y, Courville A, Bengio Y. *Deep learning*. MIT Press Cambridge; 2016.
10. Anantrasirichai N, Bull D. Artificial intelligence in the creative industries: a review. *Artif Intell Rev*. 2021. <https://doi.org/10.1007/s10462-021-10039-7>.
11. Viet N, ThanhTuyen D, Hoang T. “Parasite worm egg automatic detection in microscopy stool image based on faster r-cnn,” *Proceedings of the 3rd International Conference on Machine Learning and Soft Computing - ICMLSC*, 2019;pp. 197–202.
12. Peixinho A, Martins S, Vargas J, Falcão A, Gomes J, Suzuki C. “Diagnosis of human intestinal parasites by deep learning,” *Computational Vision and Medical Image Processing V*, 2015;pp. 107–112.
13. Li Y, Zheng R, Wu Y, Chu K, Xu Q, Sun M, Smith ZJ. A low-cost, automated parasite diagnostic system via a portable, robotic microscope and deep learning. *J Biophotonics*. 2019;12(9):e201800410.
14. Zhang J, Wang X, Ni G, Liu J, Hao R, Liu L, Liu Y, Du X, Xu F. Fast and accurate automated recognition of the dominant cells from fecal images based on faster r-cnn. *Sci Rep*. 2021;11:10361–888.
15. Razzak MI, Naz S, Zaib A. “Deep learning for medical image processing: Overview, challenges and the future,” *Classification in BioApps*, 2008;pp. 323–350.
16. Krizhevsky A, Sutskever I, Hinton G. Imagenet classification with deep convolutional neural networks. *Commun ACM*. 2017;60:84–90.
17. He K, Zhang X, Ren S, Sun J. “Deep residual learning for image recognition,” *Proceedings of the IEEE conference on computer vision and pattern recognition*, 2016;pp. 770–778.
18. Liu W, Anguelov D, Erhan D, Szegedy C, Reed S, Fu C-Y, Berg AC. “Ssd: Single shot multibox detector In: B. Leibe, J. Matas,

- N. Sebe, and M. Welling (eds) *Computer Vision – ECCV 2016*, 21–37, Springer International Publishing.
19. Ren S, He K, Girshick R, Sun J. Faster R-CNN: towards real-time object detection with region proposal networks. In: Cortes C, Lawrence N, Lee D, Sugiyama M, Garnett R, editors. *Adv Neural Inform Process Syst*. Cham: Curran Associates Inc; 2015.
 20. Bochkovskiy A, Wang C-Y, Liao H-YM. “YOLOv4: Optimal speed and accuracy of object detection,” *ArXiv*, vol. abs/2004.10934, 2020.
 21. Anantrasirichai N, Chalidabhongse TH, Palasuwan D, Naruenatthanaset K, Kobchaisawat T, Nunthanasup N, Boonpeng K, Ma X, Achim A. “Icip 2022 challenge on parasitic egg detection and classification in microscopic images: Dataset, methods and results,” in *IEEE International Conference on Image Processing (ICIP)*, 2022;pp. 4306–4310.
 22. Ronneberger O, Fischer P, Brox T. “U-Net: Convolutional Networks for Biomedical Image Segmentation,” in *International Conference on Medical Image Computing and Computer-Assisted Intervention*, 2016.
 23. Wong A, Anantrasirichai N, Chalidabhongse TH, Palasuwan D, Palasuwan A, Bull D. “Analysis of vision-based abnormal red blood cell classification,” [arXiv:2106.00389](https://arxiv.org/abs/2106.00389), 2021.

Publisher's Note Springer Nature remains neutral with regard to jurisdictional claims in published maps and institutional affiliations.